Radiochim. Acta **100**, 727–736 (2012) / **DOI** 10.1524/ract.2012.1961

Nanomaterials and nanotechnologies in nuclear energy chemistry

By W.-Q. Shi, L.-Y. Yuan, Z.-J. Li, J.-H. Lan, Y.-L. Zhao and Z.-F. Chai*

Nuclear Energy Chemistry Group, Key Laboratory of Nuclear Analytical Techniques and Key Laboratory for Biomedical Effects of Nanomaterials and Nanosafety, Institute of High Energy Physics, Chinese Academy of Sciences, Beijing 100049, China

(Received December 16, 2011; accepted in final form April 17, 2012)
(Published online July 30, 2012)

Nuclear energy chemistry / Nanomaterials and nanotechnologies / Actinides / Metal-organic frameworks / Porous materials

Summary. With the rapid growth of human demands for nuclear energy and in response to the challenges of nuclear energy development, the world's major nuclear countries have started research and development work on advanced nuclear energy systems in which new materials and new technologies are considered to play important roles. Nanomaterials and nanotechnologies, which have gained extensive attention in recent years, have shown a wide range of application potentials in future nuclear energy system. In this review, the basic research progress in nanomaterials and nanotechnologies for advanced nuclear fuel fabrication, spent nuclear fuel reprocessing, nuclear waste disposal and nuclear environmental remediation is selectively highlighted, with the emphasis on Chinese research achievements. In addition, the challenges and opportunities of nanomaterials and nanotechnologies in future advanced nuclear energy system are also discussed.

1. Introduction

With the rising global energy demand, the potential of nuclear energy, as a low-carbon energy resource, is becoming more and more obvious. But if nuclear energy is going to achieve its full potential, four grand challenges such as the maximization of application of available nuclear fuel uranium, the lifetime maximization of today's nuclear power plants, the resistance towards nuclear proliferation, and the minimization of nuclear waste *via* reasonable reprocessing and treatment must be fulfilled. New types of materials with unique behaviors and functions are considered to be central to meet all the four challenges [1].

With the emergence of the so-called nanomaterials and nanotechnology, the age has arisen in which we are able to manipulate material structures at nanometer scales, thus opening up unprecedented possibilities for designing and manufacturing new tailored functional materials. Actually, nanomaterials and nanotechnologies are expected to be capable of playing significant roles and having vast application potentials at all stages of advanced nuclear fuel cycles [2]. New capabilities in the synthesis and characterization of materials with controlled nano-scale structure offer tremendous opportunities for the development of tailored marerials for fabrication of advanced nuclear fuels (with nano-scale control of composition), use of actinides in catalysis, efficient nano-scale sorbents for spent nuclear fuel reprocessing, advanced nuclear waste forms and convenient sensors for detection of radionuclides. Therefore, some countries with developed nuclear energy programs, such as the USA, attach great importance to the research of nanomaterials and nanotechnologies; nano-scale materials research facilities have been established at six DOE (Department of Energy) national laboratories to undertake leading-edge materials development and testing [1].

It is difficult, almost impossible, to summarize all the latest important results in nanomaterials and nanotechnologies related to nuclear fuel cycle system in one short article. Thus, the advances we select for discussion are limited to nanostructured actinide materials, such as actinides encapsulated in fullerenes, uranium oxide nanocrystals, actinide nanospheres and nanoclusters, thorium and uranium based metal-organic frameworks (MOFs). Non-radioactive nanomaterials for nuclear waste disposal and environmental protection are also selectively covered in this review. In recent years, Chinese radiochemists have achieved significant success in the basic research of nanomaterials and nanotechonologies and their applications in future advanced nuclear fuel cycle. In this regard, important contributions of Chinese scientists in this field are specifically highlighted. In spite of these considerations, we hope that this article might shed light on the further research directions of the nanoscience and nanotechnology in the nuclear energy field, particularly in the nuclear fuel cycle chemistry.

2. Actinides encapsulated in fullerenes and neutron radiation-induced novel fullerenes

Fullerenes, as a new class of carbon molecules with hollow cages composed of three-connected networks of carbon atoms, such as the most common C_{60}, are regarded as the first truly molecular form of pure carbon yet isolated. Since the first demonstration of their existence in 1985, fullerenes have become a source of interest in a variety of life, space, environmental and material sciences, due to their unique structures and properties. Particularly, metal-fullerenes, *i.e.*

*Author for correspondence (E-mail: chaizf@ihep.ac.cn).

fullerenes that contain metal atoms in a cage structure, are attracting much attention in development of new functional materials for special applications. Many efforts by several investigators have focused on studies of fullerene encapsulating actinides. Guo *et al.* [3] reported the first synthesis of actinide fullerenes, in which U@C_{28} was prepared by using the laser and carbon-arc technology. C_{28} is considered as the smallest fullerene formed with substantial yields. It has an open shell ground state and behaves as a sort of hollow superatom with an effective valence of 4. Thus, stable closed-shell derivatives of C_{28} can be obtained by trapping a tetravalent atom inside the cage to make endohedral fullerenes such as U@C_{28}, with an efficiency of production being much greater than for other endohedral metallofullerenes. Akiyama *et al.* [4] studied the production of metallofullerenes for U, Np and Am. Two kinds of uranium metallofullerenes, U@C_{82} and U_2@C_{80} with uranium oxidation state of +3, were prepared by the conventional arc-discharge method, and then purified and identified by HPLC (High Performance Liquid Chromatography). Metallofullerenes for Np, and Am were also successfully obtained. From the equivalence of the HPLC retention time and similar 5 f characterizations as actinide elements, it was assumed that the major products for Np and Am fullerenes are also M@C_{82} species with the oxidation state of +3.

The studies quoted above have dealt with the synthesis of actinide endohedral fullerenes, but the detailed structures of actinides in the cage of fullerenes, however, still remain unclear. Recently, Wu and Lu [5] revealed the presence of unprecedented U−U multiple bond in U_2@C_{60} by means of all-electron relativistic density functional computations. The optimized structures and symmetries of U_2@C_{60} isomers **1a**–**d** derived from the C_{60} (I_h) fullerene are depicted in Fig. 1. The U−U multiple bond in this work is dominated by the uranium 5 f atomic orbitals and is very different from the metal-metal bonds in the d- and f-block polynuclear metal complexes. This finding may open a way for connecting the metal-metal multiple bonding and the fullerene chemistry. However, some authors give different opinions. Infante *et al.* [6], for example, suggested through a DFT study on endohedral and exohedral U_2@C_{60} systems that U−U binding found in C_{60} is a calculation artifact due to the small size of the cage. In a larger cavity such as C_{70} or C_{84}, two U atoms mainly interact with the interior wall of the cage and the U–U bond no longer exists. Anyway, the differences on the proposed structures of U atoms in C_{60} will promote further interest in endohedral fullerenes. It is reasonable to believe that the true potential for nuclear waste management using fullerenes can be realized by fostering wider attention and discussion on the actinide endohedral fullerenes.

Inspired by the successful synthesis of actinide fullerene composites, Zhao *et al.* continued to explore novel-structured fullerenes by neutron irradiation. The first highly selective reaction that produces only C_{2m}-X-C_{2n} ($m = n$ or $m \neq n$, X stands for C or O) and no C_{2m}-C_{2n} type fullerene dimer was consequently found. Utilizing a neutron irradiation method, Zhao and co-workers have synthesized C_{141}, C_{131}, C_{121}, and C_{140}O, of which C_{141} and C_{131} were prepared and characterized for the first time [7, 8]. The synthesis method is described in Fig. 2. This method is simple and capable of producing new C_{2m}-X-C_{2n} molecules by chemical

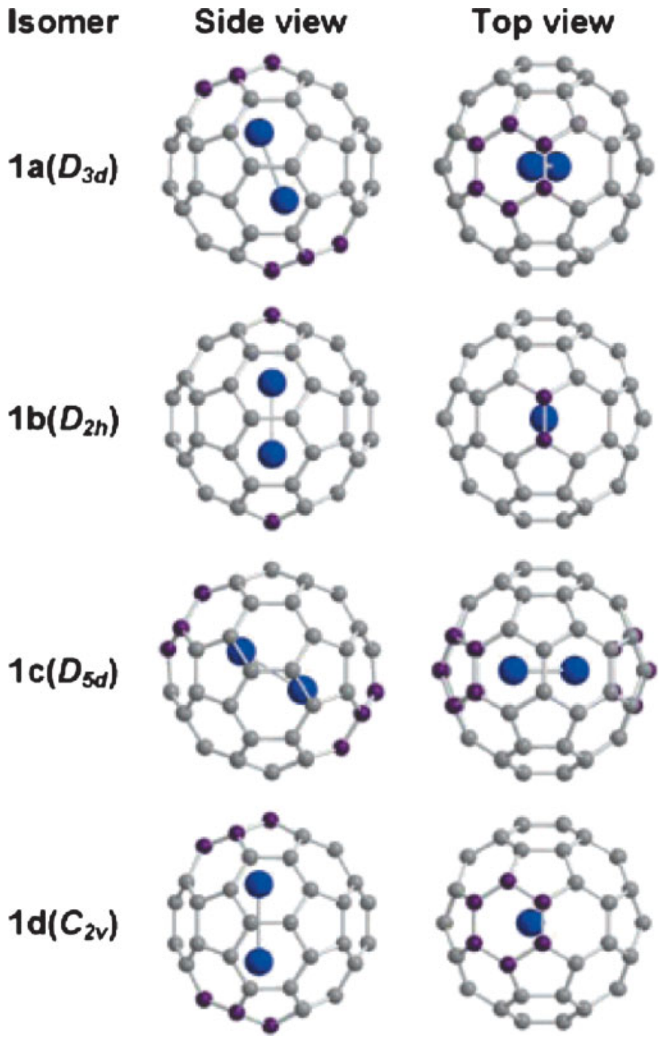

Fig. 1. Optimized structures and symmetries of U_2@C_{60} isomers derived from the IPR-satisfying C60 (I_h) fullerene. Uranium atoms are represented by large blue balls, the carbon atoms closest to uranium are colored in purple [5].

modification of precursors to introduce different X-atoms into the reaction system prior to the energetic radiation. The irradiation with neutrons of high energy could create reactive sites for covalently bound bridges between fullerenes originally only weakly bound by van der Waals forces. The results open a new direction and provide a practical approach for polymer sciences of fullerenes and fullerene derivatives.

One possible formation mechanism for C_{2m}-X-C_{2n} is proposed as follows. In the irradiation process, energetic neutrons transferred their energy to C_{70} or C_{60} cages. It caused a secondary ionization and induced a dissociation of C_{70} or C_{60} molecule to form some fragmental species as well as excited C_{70} or C_{60} cages. The reactions among excited C_{70} or C_{60} cages (of high reactivity) and nascent fragmental species hence occurred. This process finally resulted in the new molecule C_{141}.

3. Uranium-oxide nanocrystals

As it is well known, in its enriched form, uranium dioxide is the major component of nuclear fuel. When depleting its

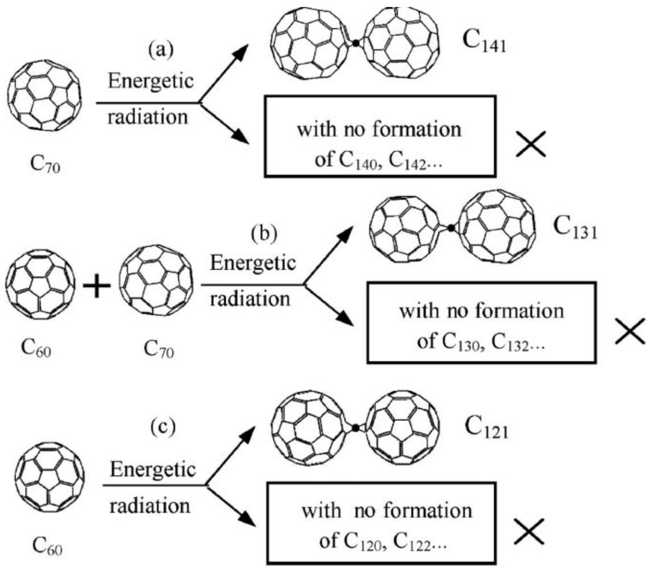

Fig. 2. The schematic synthesis routes for fullerene dimers C_{141}, C_{131}, C_{121} [8].

progenies, it is also widely used in many fields, including radiation shielding and catalysis, *etc.* Nanostructured nuclear fuel is expected to possess superior properties, therefore fabrication of nano-fuel may become a hot topic in nanoscience. Recently, Wu *el al*. [9] synthesized high quality, colloidal uranium oxide nanocrystals by thermal decomposition of uranyl acetylacetonate in a mixture solution of oleic acid (OA), oleylamine (OAm), and octadecene. This synthesis showed characteristic high reaction-yield of 75% and high reproducibility. X-ray powder diffraction (XRD) confirmed that the nanocrystals were pure uranium-dioxide. The Bragg reflections are quite distinguishable from those of the typical crystal structures of other uranium-oxides such as U_3O_8 and UO_3. The transmission electron microscopy (TEM) showed that periodical pore structures with diameters in the nanometer scale were available within the nanocrystals. It was also found that the size of the nanoparticles and the pore size could be controlled by changing the ratio of the organic additives in the reactions. This work is of high significance because this UO_2 nanocrystal could be developed as a candidate of potential nano-fuels. The evenly distributed pores might adsorb and accommodate the highly reactive fission products such as iodine which can react with the clad under extreme conditions, and then mitigate fuel-clad or other undesirable chemical interactions. Furthermore, this microstructure can hopefully enhance the thermal and radiation stability of the fuel and consequently improve its burn-up [10].

Wang *et al.* [11] synthesized sphere-shaped UO_2 nanoparticles (average diameter 100 nm) consisting of 15 nm nanocrystals and single crystalline U_3O_8 nanorods (diameter 80–100 nm and length 500–1500 nm) under hydrothermal conditions, using $UO_2(OAc)_2{\cdot}2H_2O$ and amines as both reducing and structure-directing agents. By adjusting the reaction conditions such as the volume ratio of the solvent and the reducing agent, the size and morphology of the uranium dioxide nanostructures varied to a certain degree. TEM revealed that the U_3O_8 nanorods grew along the crystallographic [001] direction. The UO_2 nanoparticles could be converted to porous U_3O_8 aggregates through thermal treatment in air. TEM images also showed the availability of irregular macropores in the aggregates, which were formed from the inter-growth of nanocrystals. A catalytic test for the oxidation of benzyl alcohol exhibited much better catalytic activity of the porous U_3O_8 aggregates than the U_3O_8 nanorods, clearly illustrating morphology-dependence of the catalytical properties. Similarly, it is reasonable to believe that porous aggregates of U_3O_8 are more preferred from nuclear fuel point of view. Another merit of porous uranium oxides might lie in their applications in the fabrication of transmutation fuel. Normally, to prevent generation and diffusion of strong radioactive dust, wet-methods are favored for the fabrication of transmutation fuel. As porous materials show substantial adsorption ability for minor actinides (MA), porous uranium oxides adsorbed with MA can then be directly fabricated into transmutation fuel. Anyway, further research is still much needed to test the application potentials of nanostructured UO_2 and U_3O_8.

4. Actinide nanoclusters and metal-organic frameworks (MOFs)

Actinide solid-state and coordination chemistry has advanced through unexpected and interesting results that have further identified the complex nature of the 5*f* elements. Nano-scale control of actinide materials has been emerging in recent years, as shown by the creation of a considerable range of actinide clusters and tubular topologies. Generally, the U(VI) species with coordination geometries such as square, pentagonal, and hexagonal bipyramids can be considered as the primary building blocks (PBUs) of uranyl inorganic extended structures (Fig. 3). Burns and his coworkers reported synthesis of 26 clusters built from uranyl peroxide polyhedra. Among them 16 contain solely uranyl polyhedra, 8 also contain pyrophosphate, and two others are inorganic-organic uranyl-oxalate hybrid materials [12–15]. There are several possible ways in which pyrophosphate or oxalate can coordinate a uranyl ion.

The sizes of the synthesized U(VI) clusters span a considerable range (1.5 ∼ 3 nm), and contain 20 ∼ 60 uranyl polyhedra [12, 13]. The specifics of the U-O_2-U dihedral angle depend upon the size and location of counter ions, with larger counter ions favoring a dihedral angle that is

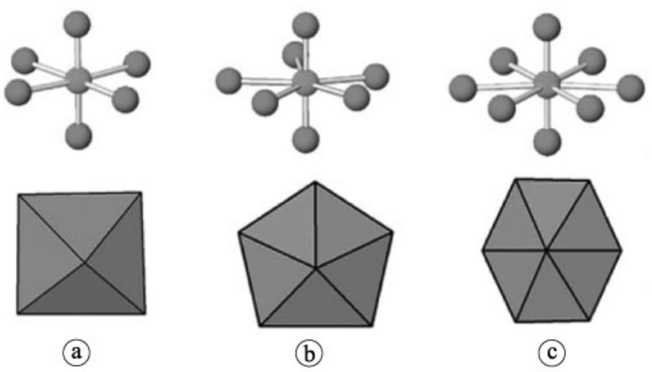

Fig. 3. Coordination polyhedra in uranyl compounds: (**a**) square bipyramid, (**b**) pentagonal bipyramid, and (**c**) hexagonal bipyramid centered by uranium atom.

closer to 180°. This dihedral angle influences the curvature of cage clusters built from uranyl polyhedra, and thus also the size of closed clusters. It is possible to tune the compositions and topologies of these nanoclusters for use as precursors in the creation of novel waste forms or nuclear fuels. Such clusters present the possibility of nanocontrol of chemical composition and properties of the materials.

Over the last ten years, the metal-organic frameworks have been widely investigated owing to their potential applications in various fields, especially in absorption and separation of organic molecules and metallic ions [16–18]. Compared to the commonly used main group and transition metal elements, actinide MOFs materials are less investigated owing to their radioactivity. However, actinide-organic frameworks may be potential novel precursors for nuclear fuel fabrication and have potential applications in nuclear waste processing. Therefore, actinide MOFs have attracted increasing attention as the nuclear energy revives in this century.

MOFs possess diverse topologies and constitutions as found previously. However, the actinide elements in actinide-organic frameworks exhibit high coordination number of 7, 8, and even 9. Therefore, the actinide-bearing MOFs built from MX_7, MX_8, and MX_9 units would display completely distinct structural characteristics. In their experiment, O'Hare *et al.* have successfully synthesized several thorium-organic frameworks, TOF-X (X = 1–3), under hydrothermal conditions [19, 20]. In 2003, the first thorium-organic framework was structurally characterized [19]. The $[(Th_2F_5)(NC_7H_5O_4)_2\ (H_2O)][NO_3]$ (TOF-1) is composed of a thorium oxyfluoride chain running along the [010] direction with cross-linking pyridinedicarboxylate (PDC) groups. Herein, the chain consists of corner-sharing thorium oxyfluoride polyhedra containing 9-coordinate thorium, with each thorium coordinated to four oxides and five fluorides. $Th[C_6H_3(CO_2)_3F]\cdot 0.3H_2O$ (TOF-2) is composed of hexagonal channels consisting of eight-coordinate ThO_6F_2 polyhedra and 1,3,5-benzenetricarboxylic acid (BTC) groups that are connected through oxygen and fluorine atoms [20]. In TOF-2, the Th^{4+} cation is bonded to two fluorine and six oxygen atoms. $Th_3F_5[(C_{10}H_{14})(CH_2CO_2)_2]_3(NO_3)$ (TOF-3) has three-dimensional thorium–organic framework structure containing ThO_4F_5 polyhedra and 1,3-adamantanediacetate linkers [21]. The amount of calculated void space in TOF-3 is only 4.3% including nitrate anions, and reaches 10.0% after the non-framework anion NO_3^- is removed. In contrast, this amount for TOF-2 is 41%, indicating a higher porosity of TOF-2.

As is well known, U(VI) forms linear uranyl ions, UO_2^{2+}, which leads to a highly anisotropic distribution of chemical bonds within its coordination polyhedral. Krivovichev *et al.* reported a new compound, $K_5[(UO_2)_3(SeO_4)_5](NO_3)(H_2O)_{3.5}$, based upon nano-scale uranyl selenate tubules. This material possesses tubules parallel to the axis that consists of corner-sharing $\{UO_7^{8-}\}$ pentagonal bipyramids and $\{SeO_4^{2-}\}$ tetrahedra [22]. However, in the strict sense, this material is just a uranium-inorganic framework material based on an organic template. To date, a series of uranyl-organic materials including 1-D chains, 2-D layers, and 3-D frameworks have been synthesized [23–42]. For example, Thuéry synthesized two uranyl-organic frameworks, $[(UO_2)_8(L_{12}H_8)]\cdot 12H_2O$ and $[Ba(H_2O)_8]_2[(UO_2)_8Ba_2(L_{12})(H_2O)_4]\cdot 8H_2O$, using (1R,3S)-(+)-camphoric acid as organic ligands [23]. These materials both crystallize in the $I4$ space group and belong to the tetragonal crystal system. In the crystal of $[(UO_2)_8(L_{12}H_8)]\cdot 12H_2O$, each uranyl ion is bound to three chelating carboxylate groups with the usual hexagonal bipyramidal environment geometry.

In China, the UOF (uranium organic-framework) materials have also been extensively studied [38–42]. Chen *et al.* have prepared a series of UOF materials under hydrothermal conditions. For example, using 1,4-naphthalenedicarboxylate (NDC) and bipyridine (bipy) ligands, they synthesized 2D polymers of $(UO_2)_8(NDC)_{12}(4,4'\text{-bipyH}_2)_3(4,4'\text{-bipyH})_3$ and $(UO_2)_3O[Ag(2,2'\text{-bipy})_2]_2(NDC)_3$, and 1D zigzag chains of $(UO_2)_2(NDC)_2(2,2'\text{-bipy})_2$ [30]. It has been found that the above three materials belong to triclinic, triclinic, and monoclinic crystal systems, which correspond to the following space groups, $P\bar{1}$, $P\bar{1}$, and $P2_1/n$, respectively. In addition, they prepared a series of 3D uranyl–organic coordination frameworks such as $(UO_2)_3(\text{v-BTC})_2(H_2O)_4$, $(UO_2)_6O(OH)(\text{m-BTC})_2(\text{m-HBTC})_2(H_2O)_2(H_3O)\cdot 6H_2O$, and $(UO_2)_2O(\text{m-BTC})[NH_2(CH_3)_2]_2\cdot H_2O$, where v-BTC = 1,2,3-benzenetricarboxylate and m-BTC = 1,2,4-benzenetricarboxylate [39]. In the above 3D frameworks, the adjacent carboxylate groups attached to the aromatic ring in the ligands result in strong steric hindrance, leading to their orientation vertical to the aromatic ring. Selecting NDC as the ligand, other two uranyl-organic coordination compounds, $UO_2(NDC)[(CH_3)_2SO)]_2$ and $[UO_2(NDC)(CH_2OH)_2]$, have also been synthesized through a volatilization method by Chen *et al.* [42] Compared to TOFs, the UOFs are featured by the linear UO_2^{2+} unit, which tends to be equatorially coordinated.

In all, the development of new actinide-organic frameworks has become a hot topic in basic actinide solid-state chemistry. However, the present investigations in this field are predominantly focused on the coordination features of thorium and uranium. It is believed that the introduction of transuranium elements into MOFs is more challenging.

5. Nanoporous materials for the separation of high level liquid waste (HLLW)

To minimize the long-term radiological risk and facilitate the management of high level liquid waste (HLLW), a partitioning of the long-lived minor actinides (MA = Am, Cm) and some specific fission products (FPs) such as Cs, Sr, Tc and the platinum group elements is much more desirable. Compared to uranium and plutonium, the minor actinides are significantly less abundant in the spent fuel, so the scale of the separation process for minor actinides from HLLW should be considerably smaller than that of a main separation process such as PUREX. Nanoporous materials based solid-phase extraction still has its advantages such as being acid and alkali resistant, high temperature enduring and radiation resistant in processing HLLW.

In order to develop a potential direct separation process for trivalent minor actinides, Wei *et al.* designed

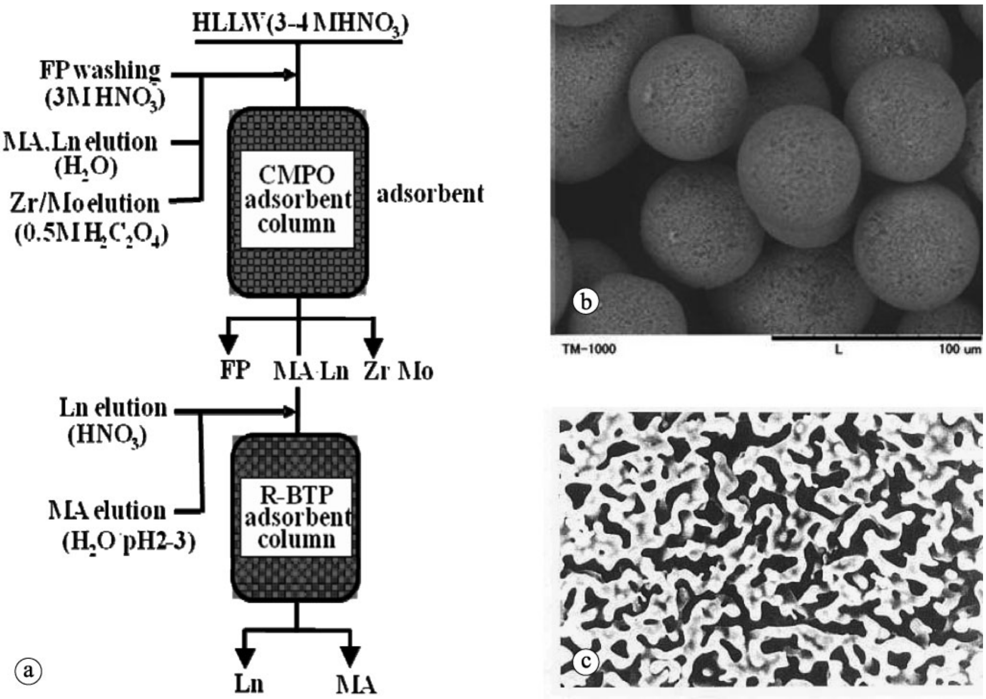

Fig. 4. The flowsheet of the MAREC process (**a**), microscopic image of *iso*hexyl-BTP/SiO_2-P (×800) (**b**), inner surface of the SiO_2 (**c**).

a novel macroporous silica-based 2,6-bis(5,6-diisohexyl)-1,2,4-triazin-3-yl)pyridine (isohexyl-BTP) extraction resin, which was prepared by impregnating isohexyl-BTP molecules into a macroreticular styrene-divinylbenzene copolymer (SiO_2-P) [43, 44]. Subsequently, the copolymer was immobilized in porous silica particles with pore size from 50 ∼ 600 nm (Fig. 4). The content of isohexyl-BTP extractant in the extraction resin (isohexyl-BTP/SiO_2-P) can be as high as 33.3 wt %. Based on the so-called functionalized macroporous silica, Wei and co-workers developed the MAREC (Minor Actinides Recovery from HLLW by Extraction Chromatography) process [44–46]. In the MAREC process, as shown in Fig. 4, two main columns packed with different extraction resins are utilized for the chromatographic separation of HLLW through selective adsorption and elution procedures. The first column is packed with CMPO/SiO_2-P (CMPO: octyl(phenyl)-*N*,*N*-diisobutylcarbamoyl-methylphosphine oxide) extraction resin and the second with R-BTP/SiO_2-P (R: alkyl group) extraction resin. The elements can be effectively separated into the following three groups in the first column depending on their different adsorption and elution behaviors which result from the complexation ability of the metal ions with CMPO: (1) Cs, Sr, Rh and Ru (non-adsorptive or weakly adsorptive FPs); (2) MA and RE (rare earth elements); (3) Zr and Mo. Subsequently, the MA-containing effluent is applied to the second column where the elements are separated to (1) RE, and (2) MA, respectively. Actually, as Am,Cm and lanthanides show similar chemical properties such trivalent oxidation state, ionic radii, and comparable hydrated ions, selective separation of trivalent actinides (An(III)) from lanthanides (Ln(III)) in high level liquid waste (HLLW) is a great challenge in industry.

With the rapid development of computer science, computational chemistry now plays a pivotal role in ligand designing and in the prediction of the affinity between ligands and central metal ions. This fact is of particular significance for MA ligand designing, because most experiments related to MA are complicated and expensive. Ligand designing and screening through quantum chemistry calculations before real experiments can be a convenient and economical approach to find highly efficient MA ligands for Ln/An separation [47, 48].

By a similar approach, Zhang *et al.* synthesized several other macroporous silica-based supramolecular recognition polymeric composites, which were modified by 1,3-[(2,4-diethyl-heptylethoxy)oxy]-2,4-crown-6-calix [4]arene (calix[4]arene-R14), (calix[4]+Oct)/SiO_2-P [49]. The *n*-octanol was used to modify calix[4]arene-R14 through hydrogen bonding. Based on the results from experiments with simulated HLLW, calix[4]tOct)/SiO_2-P showed excellent adsorption ability and high selectivity for Cs(I) at 4.0 M HNO_3 over the tested elements. The partitioning of Cs(I) from a simulated HLLW was operated by a (calix[4]tOct)/SiO_2-P packed column. Cs(I) was effectively eluted by water and separated from other investigated metals. It is demonstrated that (calix[4]tOct)/SiO2-P would be promising to be applied in chromatographic separation of Cs(I) from HLLW [50].

As shown in Fig. 5, the superior selectivity of calix[4]-arene-R14 for Cs(I) is due to the effective matching of the sizes between the calixarene cavity and Cs(I) ion, as well as π-bonding interactions with the arene groups. The ionic radii of all REEs(III) including Y(III) and La(III) to Lu(III), as well as the other FPs such as Mo(VI), Pd(II), Ru(III), Rh(III), Cs(I), and Zr(IV) are in the range of 0.0848–0.106 nm and 0.065 to 0.086 nm. The cavity size of calix[4]arene-R14 is reported to be about 0.162 nm, which is very close to that of Cs(I), 0.167 nm. So, the cavity size of calix[4]arene-R14 matches well that of Cs(I), as shown in Fig. 5. It makes the adsorption ability of Cs(I) ion onto (calix[4]tOct)/SiO2-P high, whereas the other metals show poor adsorption [49].

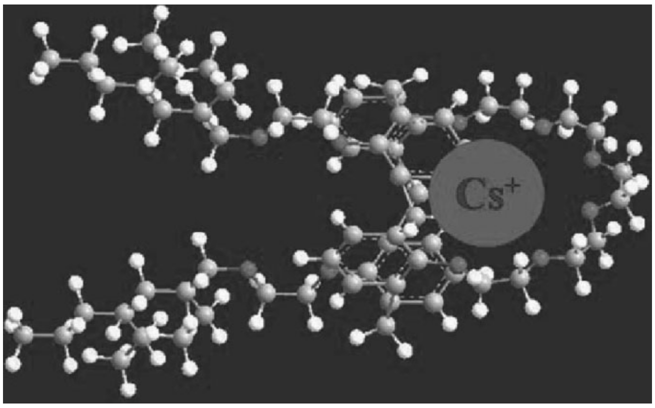

Fig. 5. Complexing formation of Cs(I) with calix[4]arene-R14 [49].

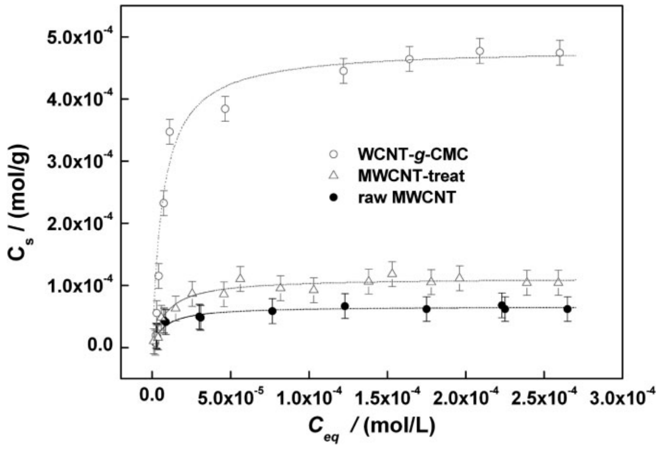

Fig. 6. Sorption isotherms of the removal of UO_2^{2+} from solution on raw MWCNT and MWCNT-g-CMC. $T = 25 \pm 2\,°C$, equilibrium time 24 h, pH $= 5.0 \pm 0.1$, $C_{[NaClO_4]} = 1.0 \times 10^{-2}$ mol/L, $m/V = 0.4$ g/L.

As the processing of HLLW normally represents harsh chemical conditions such as high nitric acid concentration and extremely high level of radiation, the chemical and radiation stability of the impregnated nanoporous silica is particularly important. According to the stability test by Wei and his co-workers [51], the silica-based support was significantly stable against γ-radiation and nitric acid. A part of R-BTP was dissolved into nitric acid solution from the extraction resin due to protonation. However, the branched R-BTP (*iso*-Bu-BTP) resin was much more stable than a normal R-BTP in nitric acid solution (≤ 3 M). Anyway, the radiation stability of the above materials still needs further evaluation by extending the experiments to α-radiation.

6. Nanomaterials for nuclear waste disposal and environment remediation

The renaissance of nuclear energy promotes increasing demands for dealing with the troublesome nuclear contamination and the diffusive high concentrated radioactive waste. Especially, after this year's Fukushima nuclear accident, a large quantity of high concentrated radioactive waste water has been discharged into the ocean, causing a great public concern. This leads to more exigent efforts in removal of radionuclides from aqueous solution for water decontamination and environmental protection. Under this situation, versatile nanomaterials that can remove the radionuclides and remediate the environment are favored by more and more investigators.

Carbon nanotubes (CNTs), as well known, are a novel and important graphitic carbon nanomaterial, and have been widely applied in various scientific areas. CNTs exhibit many noteworthy properties such as strong tensile strength, large elastic modulus, high heat conductivity and electrical conductibility and large surface area [52]. These advantages make CNTs an ideal supporting material for solid-phase extraction of radionuclides. Wang *et al.*, for example, firstly reported the sorption of lanthanides and actinides from $NaClO_4$ aqueous solution by using multiwall carbon nanotubes (MWCNTs). It was found that MWCNTs are an effective sorbent for Eu(III) [53], Am(III) [54] and Th(IV) [55, 56], and the sorbent after nuclides sorption is very stable due to the strong complexation of sorbates on the MWCNTs surface. The authors further fabricated carboxymethyl cellulose grafted MWCNT (MWCNT-g-CMC) by using plasma induced grafting method. The preliminary results suggested that MWCNT-g-CMC is easily dispersed in solution and has much higher adsorption capacity for U(VI) compared to the raw MWCNT, as shown in Fig. 6 [57]. These works highlight the vast opportunities of CNTs applied in separation of radionuclides from aqueous solutions. However, the studies performed at the Institute for Transuranium Elements (ITU) of the European Commission in Karlsruhe and the Institute of Nuclear Sciences of Ege University (INS) do not confirm this high performance of MWNTs for Th and Am (the adsorption capacity of ≤ 10 mg/g *vs.* ≥ 40 mg/g reported by Wang *et al.*). The authors attributed the difference to the pretreatment of the CNTs prior to batch sorption experiments. That is, the pretreatment will enhance the adsorption capacity of CNTs by increasing the degree of purity, providing more hydrophilic surface and increasing the amount of oxygen-bearing functional groups [52].

From a pragmatic point of view, some material issues of these nanomaterials need to be discussed first to better define the potential applications of CNTs. Basically, the reversibility of adsorption and durability mainly determine the reusability and "economics" of the CNTs. In current stage, the reports about the reusability and durability of CNTs are rare, and it is hard to say that CNTs are more appropriate candidates for environmental remediation compared to inorganic materials such as *e.g.* clay, zeolite and prussian blue sorbents. Further work is necessary to promote the adsorption capacity, selectivity and radiation stability of CNTs, making them more competitive compared to traditional adsorbents in radionuclides preconcentration and environmental remediation.

Beside CNTs, mesoporous materials, porous molecular sieves with pore diameter between 2 and 50 nm, such as SBA-15 (Santa Barbara Amorphous-15), are also important nanomaterials that have received ever-increasing attention in various scientific areas. Ordered mesoporous carbon and silica materials are novel families of the fascinating porous solids, which have the advantages of large surface area, well-defined pore size, excellent mechanical resistance, non-swelling, excellent chemical stability and radiation tolerance, as well as extraordinarily wide possibilities of functionalization [58, 59]. These advantages also make the ordered mesoporous carbon and silica compounds attractive for nuclear waste disposal.

Vidya *et al.* [60, 61] reported the entrapment of UO_2^{2+} in MCM-41 and MCM-48 molecular sieves based on direct template-ion-exchange. It was found that the entrapment of UO_2^{2+} was facilitated by the large pore size and the high surfactant content in the as-synthesized host materials. However, these sorbents normally show poor selectivity and slow sorption kinetics for UO_2^{2+}. To promote the sorption selectivity and achieve higher sorption capacity and faster sorption kinetics, mesoporous surface based functionalizations were performed. Li *et al.* [62] developed a new sorbent for U(VI) by functionalizing ordered mesoporous carbon CMK-5 with 4-acetophenone oxime (Oxime-CMK-5) *via* thermally initiated diazotization. The U(VI) sorption by Oxime-CMK-5 was also found to be very fast and pH-dependent, and a maximum U(VI) sorption capacity of 65.18 mg/g could be achieved. Fryxell and his co-workers [63, 64] developed self-assembled monolayers on mesoporous supports (SAMMS), in which organosilicates with functional moieties are orderly attached on the surface of MCM-41, as an efficient method for actinides sequestration. Yousefi *et al.* [65] studied the solid-phase extraction of U(VI) using 5-nitro-2-furaldehyde modified mesoporous silica (MCM-41). The sorbent exhibits good stability, reusability, high sorption capacity and fast rate of equilibrium for sorption/desorption of U(VI). Recently, we synthesized two kinds of organic functionalized mesoporous silicas, phosphonate functionalized MCM-41(NP10) [66] and amino functionalized SBA-15 (APSS) [67], by co-condensation and grafting method, respectively. Consequently, the synthesized materials were used as sorbents for the removal of U(VI) from aqueous solution. Fig. 7 shows the structure of NP10 and the sorption isotherm for U(VI) in NP10. It is found that U(VI) sorption has ultra-fast kinetics and the new sorbents offer large sorption capacity. The maximum sorption capacity in APSS, for example, is even more than 400 mg/g at pH 5.3 ± 0.1. Furthermore, these silica materials show a desirable selectivity for U(VI) ions over a wide range of competing metal ions. The studies on the sorption mechanism of U(VI) on the organic functionalized mesoporous silicas and on Th(IV) sorption using the organic functionalized mesoporous silicas are still underway in our laboratory.

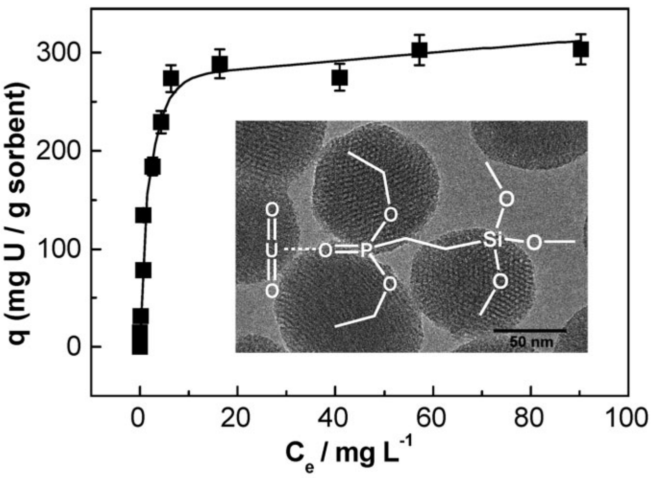

Fig. 7. Sorption isotherms of U(VI) in NP10. Equilibrium time 3 h, pH = 6.9 ± 0.1, $m/V = 0.4$ g/L. Inset shows the HRTEM image and structure of the synthesized NP10 sorbent.

In addition, magnetite nanoparticles (MNPs) have received much attention recently to remove radioactive metal ions due to the easy separation of sorbent from solution by adding a magnetic field. Xu *et al.* reported the first use of bisphosphonate modified magnetite Fe_3O_4 nanoparticles to remove UO_2^{2+} from blood. At pH 7.0, the partitioning coefficient (K_d) is estimated as high as 19.8 L/g, and the sorbent can be easily removed from blood by using a small magnet [68]. However, the Fe_3O_4 nanoparticles are unstable at acid condition, which limits their application for nuclides sorption from acid nuclear waste water. Qiang *et al.* developed silica coated magnetic nanoparticles for the separation of acidic nuclear waste, in which the Fe_2O_3 nanoparticles were coated with the silica, followed by covalent attachment of the actinide-specific chelators to separate nuclear waste under acidic conditions. The silica coated MNPs are stable even in 1 M HCl solution, and show enhanced actinide separation efficiency compared to the uncoated counterparts [69].

All above mentioned studies have dealt with radionuclides adsorption and separation using nanomaterials. From these works we could reassert that nanomaterials show several interesting aspects for application in nuclear waste disposal and environmental remediation. However, some nanomaterials are not quite stable under the conditions of ionizing radiation and can not keep their functions for relatively longer period of time in complex chemical environments. Furthermore, the issues on safety and migration behaviors of nanomaterials themselves still need clarification and evaluation. In these regards, full realization of a true potential of nanomaterials as radionuclide adsorbents requires further studies concentrating on developing high efficient, radiation-resistant, renewable and environment-friendly nanomaterials for solid-phase extraction of radionuclides.

7. Nanomaterial-based sensors for actinide cations

Within the category of sensing and detection of radionuclides, nanotechnology anticipates the capability to provide more sensitive and cost-effective techniques for detecting radioactive pollution in the air, soil, and water. Uranium is a toxic element which might be released into the environment by increasing development of nuclear energy. Severe damaging effects of uranium to human health have been reported [70, 71] and the maximum contamination level in drinking water is defined as 150 nM by US EPA [72]. Currently, uranium analysis requires expensive and complicated instruments, such as inductively coupled plasma mass spectrometry, atomic absorption and so on, which limits on-site and real-time detection of uranium. Portable metal ion sensors with high sensitivity and selectivity would serve much in future environmental monitoring. But, due to the oxycationic structure of UO_2^{2+}, it is very difficult to design a specific ligand to complex uranyl ions. As the discovery of uranyl specific DNAyme, the DNAymes have been converted into high performance fluorescent sensors using a catalytic beacon method [73]. One of them has a 45 pM detection limit and million-fold selectivity [74]. While fluorescent sensors still require instruments, *i.e.* fluorimeters, in contrast, colorimetric sensors realize simple on-site and real-time detections without any instruments, thus drawing more and more attention. Recently, Lee *et al.*[73] synthesized uranyl specific colorimetric sensors using the uranyl specific DNAymes and gold nanoparticles (AuNPs) by labeled or label-free methods. In the labeled method, the presence of UO_2^{2+} dissociated very stable DNAymes-functionalized AuNP aggregates, whose color was purple, releasing red individual AuNPs. The detection limit of this method was 50 nM after 30 min contact period. The label-free method made use of different adsorption properties of single-stranded and double-stranded DNA on AuNP. The presence of UO_2^{2+} induced the cleavage of substrate by DNAyme and the formed single-stranded DNAs can be adsorbed on the surface of AuNPs, which prevent AuNP aggregation in a NaCl solution. Detection limits were as low as 1 nM after 6 min of reaction time. Both methods exhibit much lower detection limits than the maximum contamination level in drinking water, have excellent selectivity over other metal ions, and operate at room temperature. Furthermore, the general properties of these two colorimetric sensors were systematically compared in various aspects, thus providing important guidance to facilitate researchers to choose more appropriate methods.

8. Conclusion and perspectives

The impetus of creating various novel radio-inspired nanostructures comes from the tremendous basic research needs for the future advanced nuclear energy system. This review is highlighting a variety of studies that provide new insights into the nanostructures and behaviors of solid-state actinides and novel nanomaterials, which can be used for design and fabrication of new nuclear fuels, nuclear waste disposal matrices, materials for environmental remediation, and radionuclides sensing. Most cases emphasized here were even unlikely to be anticipated a decade ago. Basically, the challenges of $5f$ electrons offer grand scientific opportunities for actinide solid-state chemistry. This trend will continue in the foreseeable future. Although it is quite difficult and expensive, breakthrough studies will heavily rely on laboratory research conducted with the real actinides, rather than experiments using chemical homologues. However, considering the complicated experimental conditions needed for actinides, actinide computational chemistry is still an essential tool to build actinides nanostructures. This range of approaches will benefit the development of a sophisticated understanding of structure-property relationships in nanoscale actinide clusters. Such an understanding will be incorporated into future attempts to design nanomaterials for specific purposes, such as applications in future advanced fuel cycles.

In all, from the above descriptions, we can definitely conclude that nanomaterials and nanotechnologies have diverse potential applications in various aspects of nuclear energy chemistry. No doubt, they will play important roles in future advanced nuclear energy systems. However, from the point of view of current international research status, nanomaterials and nanotechnologies in the field of nuclear energy are still in their infancy, there are still huge key scientific issues that should be addressed. With the deepening of the further research work, the advantages of nanomaterials and nanotechnologies will be found out step by step.

Acknowledgment. This work was supported by the National Natural Science Foundation of China (Grant No. 91026007) and the "Strategic Priority Research Program" of the Chinese Academy of Sciences (Grant No. XDA03010401 and No. XDA03010403). The authors would also like to thank Professors Yuezhou Wei, Xiangke Wang, Anyun Zhang and Ms Yalan Liu for providing valuable information. Prof. S. M. Qaim is highly acknowledged for his encouragement regarding the preparation of this manuscript.

References

1. Hill, D. J.: Nuclear energy for the future. Nature Mater. **7**, 680 (2008).
2. Basic research needs for advanced nuclear energy systems. Report of the Basic Energy Sciences Workshop, Office of Basic Energy Sciences, DOE, Washington, D.C. (2006).
3. Guo, T., Diener, M. D., Chai, Y., Alford, M. J., Haufler, R. E., McClure, S. M., Ohno, T., Weaver, J. H., Scuseria, G. E., Smalley, R. E.: Uranium stabilization of C_{28}: a tetravalent fullerene. Science **257**, 1661 (1992).
4. Akiyama, K., Zhao, Y. L., Sueki, K., Tsukada, K., Haba, H., Nagame, Y., Kodama, T., Suzuki, S., Ohtsuki, T., Sakaguchi, M., Kikuchi, K., Katada, M., Nakahara, H.: Isolation and characterization of light actinide metallofullerenes. J. Am. Chem. Soc. **123**, 181 (2001).
5. Wu, X., Lu, X.: Dimetalloendofullerene U-2@C-60 has a U−U multiple bond consisting of sixfold one-electron-two-center bonds. J. Am. Chem. Soc. **129**, 2171 (2007).
6. Infante, I., Gagliardi, L., Scuseria, G. E.: Is fullerene C-60 large enough to host a multiply bonded dimetal? J. Am. Chem. Soc. **130**, 7459 (2008).
7. Chen, Z. L., Zhao, Y. L., Qu, L., Gao, X. F., Zhang, J., Yuan, H., Chai, Z. F., Xing, G. M., Cheng, Y.: Synthesis of new carbon nanomolecule: C_{141}. Chin. Sci. Bull. **49**, 793(2004).
8. Zhao, Y. L., Chen, Z. L., Yuan, H., Gao, X. F., Qu, L., Chai, Z. F., Xing, G. M., Yoshimoto, S., Tsutsumi, E., Itaya, K.: Highly selective and simple synthesis of C2m-X-C2n fullerene dimers. J. Am. Chem. Soc. **126**, 11134(2004).
9. Wu, H., Yang, Y., Cao, Y. C.: Synthesis of colloidal uranium-dioxide nanocrystals. J. Am. Chem. Soc. **128**, 16522 (2006).
10. Mantoura, S.: Uranium dioxide: nano goes nuclear. Nature Nanotech. DOI 10.1038/nnano.2006.202 (2006).
11. Wang, Q., Li, G. D., Xu, S., Li, J. X., Chen, J. S.: Synthesis of uranium oxide nanoparticles and their catalytic performance for benzyl alcohol conversion to benzaldehyde. J. Mater. Chem. **18**, 1146 (2008).
12. Burns, P. C., Ikeda, Y., Czerwinski, K.: Advances in actinide solid-state and coordination chemistry. MRS Bull. **35**, 868 (2010).
13. Burns, P. C.: Nanoscale uranium-based cage clusters inspired by uranium mineralogy. Mineral Mag. **75**, 1 (2011).
14. Ling, J., Qiu, J., Sigmon, G., Ward, M., Szymanowski, J. E. S., Burns, P. C.: Uranium pyrophosphate/methylenediphosphonate polyoxometalate clusters. J. Am. Chem. Soc. **132**, 13395 (2010).
15. Ling, J., Wallace, C., Szymanowski, J. E. S., Burns, P. C.: Hybrid uranium-oxalate fullergy cage clusters. Angew. Chem. Int. Ed.**49**, 7271 (2010).
16. Seo, J. S., Whang, D., Lee, H., Jun, S. I., Oh, J., Jeon, Y. J., Kim, K.: A homochiral metal-organic porous material for enantioselective separation and catalysis. Nature **404**, 982(2000).
17. Férey, G., Latroche, M., Serre, C., Loiseau, T.: Hydrogen adsorption in the nanoporous metal-benzenedicarboxylate M(OH)(O_2C-

C_6H_4-CO_2) (M = Al^{3+}, Cr^{3+}), MIL-53. Chem. Commun. **24**, 2976 (2003).
18. James, S. L.: Metal-organic frameworks. Chem. Soc. Rev. **32**, 276 (2003).
19. Kim, J. Y., Norquist, A. J., O'Hare, D.: $[(Th_2F_5))(NC_7H_5O_4)_2(H_2O)][NO_3]$: An actinide-organic open framework. J. Am. Chem. Soc. **125**, 12688 (2003).
20. Ok, K. M., Sung, J., Hu, G., Jacobs, R. M. J., O'Hare, D.: TOF-2: A large 1D channel thorium organic framework. J. Am. Chem. Soc. **130**, 3762 (2008).
21. Ok, K. M., O'Hare, D.: Synthesis, structure, and characterization of a new thorium-organic framework material, $Th_3F_5[(C_{10}H_{14})(CH_2CO_2)2]_3(NO_3)$. Dalton Trans. **41**, 5560 (2008).
22. Krivovichev, S. V., Kahlenberg, V., Kaindl, R., Mersdorf, E., Tananaev, I. G., Myasoedov, B. F.: Nanoscale tubules in uranyl selenates. Angew. Chem. Int. Ed. **44**, 1134 (2005).
23. Kim, J. Y., Norquist, A. J., O'Hare, D.: Incorporation of uranium(VI) into metal-organic framework solids, $[UO_2(C_4H_4O_4)]\cdot H_2O$, $[UO_2F(C_5H_6O_4)]\cdot 2H_2O$, and $[(UO_2)_{1.5}(C_8H_4O_4)_2]_2[(CH_3)_2NCOH_2]\cdot H_2O$. Dalton Trans. **14**, 2813 (2003).
24. Borkowski, L. A., Cahill, C. L.: Topological evolution in uranyl dicarboxylates: Synthesis and structures of one-dimensional $UO_2(C_6H_8O_4)(H_2O)(2)$ and three-dimensional $UO_2(C_6H_8O_4)$. Inorg. Chem. **42**, 7041 (2003).
25. Frisch, M., Cahill, C. L.: Syntheses, structures and fluorescent properties of two novel coordination polymers in the U-Cu-H(3)pdc system. Dalton Trans. **8**, 1518 (2005).
26. Thuéry, P.: Uranyl ion complexation by citric and tricarballylic acids: hydrothermal synthesis and structure of two- and three-dimensional uranium-organic frameworks. Chem. Commun. **8**, 853 (2006).
27. Thuéry, P.: Solvothermal synthesis and crystal structure of uranyl complexes with 1,1-cyclobutanedicarboxylic and (1R,3S)-(+)-camphoric acids – novel chiral uranyl-organic frameworks. Eur. J. Inorg. Chem. **18**, 3646 (2006).
28. Borkowski, L. A., Cahill, C. L.: Crystal engineering with the uranyl cation, I. aliphatic carboxylate coordination polymers: synthesis, crystal structures, and fluorescent properties. Cryst. Growth. Des. **6**, 2241 (2006).
29. Borkowski, L. A., Cahill, C. L.: Crystal engineering with the uranyl cation II. Mixed aliphatic carboxylate/aromatic pyridyl coordination polymers: synthesis, crystal structures, and sensitized luminescence. Cryst. Growth. Des. **6**, 2248 (2006).
30. Go, Y. B., Wang, X., Jacobson, A.: (6,3)-Honeycomb structures of uranium(VI) benzenedicarboxylate derivatives: the use of noncovalent interactions to prevent interpenetration. Inorg. Chem. **46**, 6594 (2007).
31. Frisch, M., Cahill, C. L. J.: *In situ* ligand synthesis with the UO_2^{2+} cation under hydrothermal conditions. J. Solid State Chem. **180**, 2597 (2007).
32. Knope, K. E., Cahill, C. L.: Hydrothermal synthesis of a novel uranium oxalate/glycolate *via in-situ* ligand formation. Inorg. Chem. **46**, 6607 (2007).
33. Thuéry, P.: Reaction of uranyl nitrate with carboxylic diacids under hydrothermal conditions. crystal structure of complexes with L(+)-tartaric and oxalic acids. Polyhedron. **26**, 101 (2007).
34. Thuéry, P.: Uranyl ion complexation by citric and citramalic acids in the presence of diamines. Inorg. Chem. **46**, 2307 (2007).
35. Thuéry, P.: Uranyl citrate dimers as guests in a copper–bipyridine framework: a novel heterometallic inorganic–organic hybrid compound. Cryst. Eng. Commun. **9**, 357 (2007).
36. Thuéry, P.: Novel two-dimensional uranyl–organic assemblages in the citrate and D(–)-citramalate families. Cryst. Eng. Commun. **10**, 79 (2008).
37. Thuéry, P., Masci, B.: Uranyl-organic frameworks with 1,2,3,4-butanetetracarboxylate and 1,2,3,4-cyclobutanetetracarboxylate ligands. Cryst. Growth. Des. **8**, 3430 (2008).
38. Deng, D. L., Zhang, X. F., Qian, C. T., Sun, J., Zheng, P. J., Chen, J.: A new approach for stabilizing organouranium dichloride: Synthesis and X-ray structure of $(MeOCH_2CH_2C_5H_4)_2UCl_2$. Chin. Chem. Lett. **7**, 1143 (1996).
39. Liao, Z. L., Li, G. D., Bi, M. H., Chen, J. S.: Preparation, structures, and photocatalytic properties of three new uranyl-organic assembly compounds. Inorg. Chem. **47**, 4844 (2008).
40. Liao, Z. L., Li, G. D., Wei, X. A., Yu, Y., Chen, J. S.: Construction of three-dimensional uranyl-organic frameworks with benzenetricarboxylate ligands. Eur. J. Inorg. Chem. **24**, 3780 (2010).
41. Wang, K. X., Chen, J. S.: Extended structures and physicochemical properties of uranyl-organic compounds. Acc. Chem. Res. **44**, 531 (2011).
42. Xia, Y., Wang, K. X., Chen, J. S.: Synthesis, structure characterization and photocatalytic properties of two new uranyl naphthalene-dicarboxylate coordination polymer compounds. Inorg. Chem. Commun. **13**, 1542 (2010).
43. Hoshi, H., Wei, Y. Z., Kumagai, M., Asakura, T., Morita, Y.: Separation of trivalent actinides from lanthanides by using R-BTP resins and stability of R-BTP resin. J. Alloys Compd. **408**, 1274 (2006).
44. Wei, Y. Z., Zhang, A. Y., Kumagai, M., Watanabe, M., Hayashi, N.: Development of the MAREC process for HLLW partitioning using a novel silica-based CMPO extraction resin. J. Nucl. Sci. Technol. **41**, 315(2004).
45. Wei, Y. Z., Kumagai, M., Takashima, Y., Modolo, G., Odoj, R.: Studies on the separation of minor actinides from high-level wastes by extraction chromatography using novel silica-based extraction resins. Nucl. Technol. **132**, 413 (2000).
46. Usuda, S., Liu, R. Q., Wei, Y. Z., Xu, Y. L., Yamazaki, H., Wakui, Y.: Evaluation study on properties of a novel R-BTP extraction resin – from a viewpoint of simple separation of minor actinides. J. Ion Exch. **21**, 35 (2010).
47. Lan, J. H., Shi, W. Q., Yuan, L. Y., Zhao, Y. L., Li, J., Chai, Z. F.: Trivalent actinide and lanthanide separations by tetradentate nitrogen ligands: a quantum chemistry study. Inorg. Chem. **50**, 9230 (2011).
48. Lan, J. H., Shi, W. Q., Yuan, L. Y., Feng, Y. X., Zhao, Y. L., Chai, Z. F.: Thermodynamic study on the complexation of Am(III) and Eu(III) with tetradentate nitrogen ligands: a probe of complex species and reactions in aqueous solution. J. Phys. Chem. A **116**, 504 (2012).
49. Zhang, A. Y., Hu, Q. H., Chai, Z. F.: Synthesis of a novel macroporous silica-calix[4]arene-crown polymeric composite and its adsorption for alkali metals and alkaline-earth metals. Ind. Eng. Chem. Res. **49**, 2047 (2010).
50. Zhang, A. Y., Hu, Q. H., Chai, Z. F.: Chromatographic partitioning of cesium by a macroporous silica-calix[4]arene-crown supramolecular recognition composite. Am. Inst. Chem. Eng. J. **56**, 2632 (2010).
51. Hoshi, H., Wei, Y. Z., Kumagai, M., Asakura, T., Morita, Y.: Separation of trivalent actinides from lanthanides by using R-BTP resins and stability of R-BTP resin. J. Alloys. Compd. **408**, 1274 (2006).
52. Belloni, F., Kuetahyali, C., Rondinella, V. V., Carbol, P., Wiss, T., Mangione, A.: Can carbon nanotubes play a role in the field of nuclear waste management? Environ. Sci. Technol. **43**, 1250 (2009).
53. Tan, X. L., Xu, D., Chen, C. L., Wang, X. K., Hu, W. P.: Adsorption and kinetic desorption study of $^{152+154}$Eu(III) on multiwall carbon nanotubes from aqueous solution by using chelating resin and XPS methods. Radiochim. Acta **96**, 23 (2008).
54. Wang, X. K., Chen, C. L., Hu, W. P., Ding, A. P., Xu, D., Zhou, X.: Sorption of ^{243}Am(III) to multiwall carbon nanotubes. Environ. Sci. Technol. **39**, 2856 (2005).
55. Chen, C. L., Li, X. L., Zhao, D. L., Tan, X. L., Wang, X. K.: Adsorption kinetic, thermodynamic and desorption studies of Th(IV) on oxidized multi-wall carbon nanotubes. Colloids Surf. A **302**, 449 (2007).
56. Chen, C. L., Li, X. L., Wang, X. K.: Application of oxidized multi-wall carbon nanotubes for Th(IV) adsorption. Radiochim. Acta **95**, 261 (2007).
57. Wang, X. K., Shao, D. D., Jiang, Z. Q., Li, J. X., Meng, Y. D.: Plasma induced grafting carboxymethyl cellulose on multiwalled carbon nanotubes for the removal of UO_2^{2+} from aqueous solution. J. Phys. Chem. B **113**, 860 (2009).
58. Darmstadt, H., Roy, C., Kaliaguine, S., Kim, T. W., Ryoo, R.: Surface and pore structures of CMK-5 ordered mesoporous carbons by adsorption and surface spectroscopy. Chem. Mater. **15**, 3300 (2003).

59. Lee, J. F., Thirumavalavan, M., Wang, Y. T., Lin, L. C.: Monitoring of the structure of mesoporous silica materials tailored using different organic templates and their effect on the adsorption of heavy metal ions. J. Phys. Chem. C **115**, 8165 (2011).
60. Vidya, K., Dapurkar, S. E., Selvam, P., Badamali, S. K., Gupta, N. M.: The entrapment of UO_2^{2+} in mesoporous MCM-41 and MCM-48 molecular sieves. Micropor. Mesopor. Mater. **50**, 173 (2001).
61. Vidya, K., Gupta, N. M., Selvam, P.: Influence of pH on the sorption behaviour of uranyl ions in mesoporous MCM-41 and MCM-48 molecular sieves. Mater. Res. Bull. **39**, 2035 (2004).
62. Li, S. J., Tian, G., Geng, J. X., Jin, Y. D., Wang, C. L., Li, S. Q., Chen, Z., Wang, H., Zhao, Y. S.: Sorption of uranium(VI) using oxime-grafted ordered mesoporous carbon CMK-5. J. Hazard. Mater. **190**, 442 (2011).
63. Fryxell, G. E., Lin, Y. H., Fiskum, S., Birnbaum, J. C., Wu, H., Kemner, K., Kelly, S.: Actinide sequestration using self-assembled monolayers on mesoporous supports. Environ. Sci. Technol. **39**, 1324 (2005).
64. Lin, Y. H., Fiskum, S. K., Yantasee, W., Wu, H., Mattigod, S. V., Vorpagel, E., Fryxell, G. E., Raymond, K. N., Xu, J. D.: Incorporation of hydroxypyridinone ligands into self-assembled monolayers on mesoporous supports for selective actinide sequestration. Environ. Sci. Technol. **39**, 1332 (2005).
65. Yousefi, S. R., Ahmadi, S. J., Shemirani, F., Jamali, M. R., Salavati-Niasari, M.: Simultaneous extraction and preconcentration of uranium and thorium in aqueous samples by new modified mesoporous silica prior to inductively coupled plasma optical emission spectrometry determination. Talanta **80**, 212 (2009).
66. Yuan, L. Y., Liu, Y. L., Shi, W. Q., Liu, Y. L., Lan, J. H., Zhao, Y. L., Chai, Z. F.: High performance of phosphonate-functionalized mesoporous silica for U(VI) sorption from aqueous solution. Dalton Trans. **40**, 7446 (2011).
67. Liu, Y. L., Yuan, L. Y., Yuan, Y. L., Lan, J. H., Li, Z. J., Feng, Y. X., Zhao, Y. L., Chai, Z. F., Shi, W. Q.: A high efficient sorption of U(VI) from aqueous solution using amino-functionalized SBA-15. J. Radioanal. Nucl. Chem. **292**, 823 (2012).
68. Wang, L., Yang, Z. M., Gao, J. H., Xu, K. M., Gu, H. W., Zhang, B., Zhang, X. X., Xu, B.: A biocompatible method of decorporation: Bisphosphonate-modified magnetite nanoparticles to remove uranyl ions from blood. J. Am. Chem. Soc. **128**, 13358 (2006).
69. Han, H., Johnson, A., Kaczor, J., Kaur, M., Paszczynski, A., Qiang, Y.: Silica coated magnetic nanoparticles for separation of nuclear acidic waste. J. Appl. Phys. **107**, 09B520 (2010).
70. Craft, E., Abu-Qare, A., Flaherty, M., Garofolo, M., Rincavage, H., Abou-Donia, M. J.: Depleted and natural uranium: chemistry and toxicological effects. Toxicol. Environ. Health B Crit. Rev. **7**, 297 (2004).
71. Zhou, P., Gu, B.: Extraction of oxidized and reduced forms of uranium from contaminated soils: effects of carbonate concentration and pH. Environ. Sci. Technol. **39**, 4435 (2005).
72. Wei, H., Li, B., Li, J., Dong, S., Wang, E.: DNAzyme-based colorimetric sensing of lead (Pb^{2+}) using unmodified gold nanoparticle probes. Nanotechnology **19**, 095501 (2008).
73. Lee, J. H., Wang, Z., Liu, J., Lu, Y.: Highly sensitive and selective colorimetric sensors for uranyl (UO_2^{2+}): Development and comparison of labeled and label-free DNAzyme-gold nanoparticle systems. J. Am. Chem. Soc. **130**, 14217 (2008).
74. Liu, J., Brown, A. K., Meng, X., Cropek, D. M., Istok, J. D., Watson, D. B., Lu, Y.: Catalytic beacon sensor for uranium with parts-per-trillion sensitivity and millionfold selectivity. Proc. Natl. Acad. Sci. USA **104**, 2056 (2007).